Mamba in Speech: Towards an Alternative to Self-Attention

Xiangyu Zhang[†], Qiquan Zhang[†], Hexin Liu[†], Tianyi Xiao, Xinyuan Qian, Beena Ahmed *Member, IEEE*, Eliathamby Ambikairajah *Senior Member, IEEE*, Haizhou Li *Fellow, IEEE*, Julien Epps *Senior Member, IEEE*,

Abstract-Transformer and its derivatives have achieved success in diverse tasks across computer vision, natural language processing, and speech processing. To reduce the complexity of computations within the multi-head self-attention mechanism in Transformer, Selective State Space Models (i.e., Mamba) were proposed as an alternative. Mamba exhibited its effectiveness in natural language processing and computer vision tasks, but its superiority has rarely been investigated in speech signal processing. This paper explores solutions for applying Mamba to speech processing by discussing two typical speech processing tasks: speech recognition, which requires semantic and sequential information, and speech enhancement, which focuses primarily on sequential patterns. The experimental results show the superiority of bidirectional Mamba (BiMamba) for speech processing to vanilla Mamba. Moreover, experiments demonstrate the effectiveness of BiMamba as an alternative to the self-attention module in Transformer and its derivates, particularly for the semantic-aware task. The crucial technologies for transferring Mamba to speech are then summarized in ablation studies and the discussion section to offer insights for future research.

Index Terms—Speech Recognition, Speech Enhancement

I. INTRODUCTION

Transformer-based models [1] have shone brightly across various domains in machine learning, including computer vision (CV) [2], [3], [4], natural language processing (NLP) [5], [6], [7], and speech processing [8], [9], [10], [11]. This success is linked to the multi-head self-attention (MHSA) module, which facilitates the representation of intricate data structures within a specific context window. However, the selfattention mechanism encounters a challenge with computational complexity, which grows quadratically as the size of the context window increases. In speech tasks, the window typically encompasses an entire speech signal. This particularly yields a long context especially for frame-level acoustic feature sequences, leading to a considerable increase in computational complexity. Numerous efforts have been made to address this challenge, with one notable approach being the utilization of a state space model (SSM). SSM-based approaches [12], [13], [14], [15] have been developed to handle sequential data across diverse tasks and modalities. By integrating a time-varying

Code can be found in https://github.com/Tonyyouyou/Mamba-in-Speech

Xiangyu Zhang, Qiquan Zhang, Beena Ahmed, Eliathamby Ambikairajah, Julien Epps are with the School of Electrical Engineering and Telecommunications, University of New South Wales, Sydney, Australia.

Hexin Liu, Tianyi Xiao are with the College of Computing and Data Science, Nanyang Technological University, Singapore.

Xinyuan Qian is with the University of Science and Technology Beijing Haizhou Li is with the National University of Singapore and Chinese University of Hong Kong, Shenzhen mechanism into SSMs, a selective SSM named Mamba [16] has been proposed and shown outstanding performance to be effective in CV [17], [18] and NLP [19].

However, in the field of speech processing, despite some attempts to replace Transformers with Mamba [20], [21], [22], the results have not been as satisfactory as expected. In [20], each Mamba is directly employed as a substitute for a Transformer within a dual-path framework for speech separation. [21] proposed SPMamba for speech separation, where Mamba is used in conjunction with MHSA. Although these approaches achieve high performance by employing a dual-path strategy or combining Mamba with attention to form a new module, these methods negate the low time complexity of Mamba. In the domain of multi-channel speech enhancement, Mamba was implemented to enhance a SpatialNet from offline to online [22] yet underperformed the vanilla version.

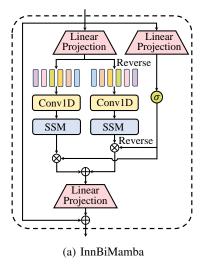
Since different speech tasks focus on various characteristics of a speech signal (e.g., speaker, language, emotion), they generally require different levels of information. However, existing approaches have mostly investigated speech enhancement and separation tasks, which focus primarily on the low-level information within a speech signal. Therefore, it is still unclear how to efficiently employ Mamba for other speech tasks, such as speech recognition and spoken language understanding, which require high-level semantic information within the speech signals.

In this paper, we explore solutions for applying Mamba to different speech tasks based on their varying information requirements (in different abstraction levels [23]) using speech recognition and speech enhancement as examples. Our research first proposes and compares two bidirectional Mamba (Bi-Mamba) structures, being external BiMamba (ExtBiMamab) and inner BiMamba (InnBiMamba). Experiments suggest that a bidirectional design can enhance the capability of Mamba to model global dependencies within the features of a speech signal. Mamba and BiMamba models are then evaluated independently or as replacements for MHSA in Transformer and Conformer models across multiple datasets. We demonstrate that the proposed BiMamba modules require additional nonlinearity to learn high-level semantic information in speech tasks, serving as an alternative to MHSA is thus an optimal approach to apply Mamba in this scenario.

II. PRELIMINARY

The State Space Model (SSM) based approaches, including the Structured State Space Sequence Model (S4) [13]

[†] Equal contribution



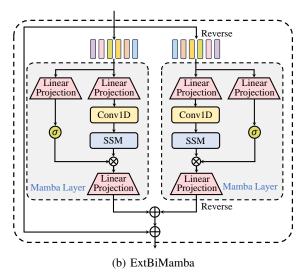


Fig. 1: The illustrations of (a) inner bidirectional Mamba (InnBiMamba) from Vison Mamba [17], and (b) the external bidirectional Mamba (ExtBiMamba). σ denotes the SiLU activation.

and Mamba [16], are derived from continuous systems. S4 facilitates the transformation of a one-dimensional function or sequence, $x(t) \in \mathbb{R}$ to $y(t) \in \mathbb{R}$, through an intermediate state h(t) in \mathbb{R}^n . The process leverages A from $\mathbb{R}^{N \times N}$ as the evolution matrix and B from $\mathbb{R}^{D \times N}$, C from $\mathbb{R}^{D \times N}$ as the input and output mapping matrices, respectively.

The fundamental equations are represented as:

$$h'(t) = Ah(t) + Bx(t), \quad y(t) = Ch(t) + Dx(t).$$
 (1)

In their discrete forms, parameter D can be represented as the residual connection in Neural Network, S4 and Mamba introduce a scaling parameter Δ , transforming the continuous matrices A,B into the discrete matrices \tilde{A},\tilde{B} respectively. This transformation commonly utilizes the Zero-Order Hold (ZOH) method, defined by:

$$\tilde{A} = \exp \Delta A, \quad \tilde{B} = (\Delta A)^{-1} (\exp \Delta A - I) \Delta B.$$
 (2)

Consequently, with the discretization into \tilde{A}, \tilde{B} , the equation (1) is adjusted for a discrete timestep Δ , given as:

$$h_t = \tilde{A}h_{t-1} + \tilde{B}x_t, \quad y_t = Ch_t. \tag{3}$$

The model then computes the final output from convolution via

$$y = x * \overline{K}, \quad \overline{K} = (C\widetilde{B}, C\widetilde{AB}, C\widetilde{A}^{L-1}\widetilde{B})$$
 (4)

The A matrix, as described above, is commonly initialized with a HiPPO matrix [24] or a Diagonal matrix [14] to adeptly capture long-range dependencies. Mamba enhances S4 by integrating a time-varying mechanism, which enlarges the dimensions of matrices B and C to $\mathbb{R}^{B \times L \times N}$, and modifies \tilde{A} and \tilde{B} to $\mathbb{R}^{B \times L \times D \times N}$.

Although these modifications have enhanced model performance, granting it "selective" capabilities, they do not alter the inherent nature of SSMs, which operate in a unidirectional manner such as RNNs [25], [26]. This is not an issue in training large language models, as many of these models are trained in an autoregressive manner [27], [28]. However, for

non-autoregressive speech models, we require a module with non-causal capabilities similar to attention. Thus, finding a suitable method to address this issue is essential. Moreover, the observation that Mamba's A matrix randomization and real-valued diagonal initialization perform equivalently suggests that Mamba's ability to delineate dependencies between inputs, compared to S4, needs further enhancement.

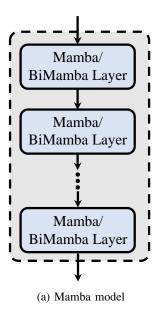
III. INVESTIGATING MAMBA IN SPEECH PROCESSING

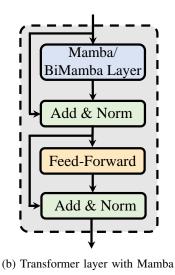
A. Bidirecional processing

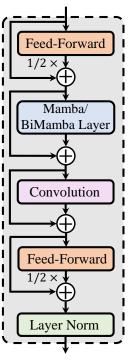
The original Mamba performs causal computations in a unidirectional manner, using only historical information. However, in speech tasks, the model is provided with the complete speech signal. Therefore, Mamba requires bidirectional computations, as employed in the MHSA module, to capture global dependencies within the features of the input signal. In this paper, we explored two bidirectional strategies for Mamba in speech tasks, i.e., inner bidirectional Mamba (InnBiMamba) from vision Mamba [17] and external bidirectional Mamba (ExtBiMamba) as shown in Figure 1.

Inner Bidirectional Layer (InnBiMamba) We first explore the inner bidirectional Mamba (InnBiMamba) from Vision Mamba [17] for speech tasks as detailed in Figure 1a. Here, two SSM modules share the same input and output projection layers. The process feeds the input forward into one SSM module, while reversing the input along the time dimension before feeding it into the other SSM module. The output of the backward SSM module is reversed back before being combined with the output of the forward SSM module. The combined output then passes through the output projection layer.

External Bidirectional Layer (ExtBiMamba) In addition, we also propose a simpler and more straight bidirectional modeling strategy, i.e., external bidirectional Mamba (ExtBi-Mamba). Unlike the InnBiMamba layer, the ExtBiMamba layer involves different input and output projection layers in forward and backward Mamba layers, respectively, as illustrated in Figure 1b. The input is fed into the forward Mamba layer and







(c) Conformer layer with Mamba

Fig. 2: Three applications of the Mamba layer in speech processing include: (a) using stacked unidirectional/bidirectional Mamba layers as an alternative to Transformer layers; (b) replacing causal and non-causal MHSA in Transformer layer with unidirectional/bidirectional Mamba; and (c) replacing MHSA in Conformer layer with the Mamba layer.

the backward Mamba layer processes the reversed input. The outputs of two Mamba layers are fused with addition operation and a residual connection is applied around the ExtBiMamaba layer. Detailed algorithms of these two methods are included in Section III-C

B. Task-aware model designs

Recent works have investigated Mamba in speech separation and speech enhancement. These tasks primarily focus on low-level spectral information of a speech signal [11]. In contrast, other speech tasks like speech recognition and spoken language understanding require capturing high-level semantic information. With reference to equation 3, SSM comprises mostly linear computations. This implies that it has limited capability to capture high-level information such as semantics and emotions. Although SiLU is used within residual structures in practical implementations, this is primarily to represent the parameter D in equation 1 for the state space model [16]. Therefore, adding more nonlinearity ability is crucial for Mamba to capture high-level information.

To capture information of various abstraction levels, we progressively explored three structures for increasing nonlinearity capability. As depicted in Figure 2a, the first strategy uses the Mamba/BiMamba layers independently (i.e., as a direct replacement for the transformer layer) to construct the Mamba/BiMamba model. The second approach employs the Mamba/BiMamba layer to replace the MHSA modules within the Transformer, where the feed-forward net (FFN) and layernorm modules are used to provide nonlinearity. The third

replaces the MHSA modules with Mamba/BiMamba layers in the Conformer, which is a variant of the Transformer employing a convolutional layer after each MHSA designed to additionally capture local information.

C. Algorithms of Bidirectional Mamba modules

Algorithm 1 InnBiMamba Layer Workflow

```
Require: \mathbf{H}_{l-1}: (B, L, D)
Ensure: \mathbf{H}_l: (B, L, D)
   1: \mathbf{H}'_{l-1}: (B, L, D) \leftarrow \mathbf{Norm}(\mathbf{H}_{l-1})
   2: \mathbf{x}: (B, L, E) \leftarrow Linear \mathbf{x}(\mathbf{H}'_{l-1})
   3: \mathbf{z}: (\mathsf{B}, \mathsf{L}, \mathsf{E}) \leftarrow \mathbf{Linear}^{\mathbf{z}}(\mathbf{H}'_{l-1})
   4: for o \in \{\text{forward}, \text{backward}\}\ do
                \mathbf{x}_o': (B, L, E) \leftarrow SiLU(Conv1d<sub>o</sub>(\mathbf{x}))
                \begin{aligned} \mathbf{B}_o: & (\texttt{B}, \texttt{L}, \texttt{N}) \leftarrow \mathbf{Linear}_o^{\mathbf{B}}(\mathbf{x}_o') \\ \mathbf{C}_o: & (\texttt{B}, \texttt{L}, \texttt{N}) \leftarrow \mathbf{Linear}_o^{\mathbf{C}}(\mathbf{x}_o') \end{aligned}
                 \Delta_o: (B, L, E) \leftarrow \log(1 + \exp(\operatorname{Linear}_o^{\Delta}(\mathbf{x}_o') +
                 Parameter_{o}^{\Delta}))
                 \overline{\mathbf{A}}_o: (B, L, E, N) \leftarrow \mathbf{\Delta}_o \otimes \mathbf{Parameter}_o^{\mathbf{A}}
                 \overline{\mathbf{B}}_o: (B, L, E, N) \leftarrow \mathbf{\Delta}_o \bigotimes \mathbf{B}_o
 10:
                 \mathbf{y}_o: (\mathsf{B}, \mathsf{L}, \mathsf{E}) \leftarrow \mathbf{SSM}\left(\overline{\mathbf{A}}_o, \overline{\mathbf{B}}_o, \mathbf{C}_o\right)(\mathbf{x}_o')
 11:
 12: end for
 13: y'_{\text{forward}}: (B, L, E) \leftarrow y_{\text{forward}} \odot \text{SiLU}(\mathbf{z})
 14: y'_{\text{backward}}: (B, L, E) \leftarrow y_{\text{backward}} \odot \text{SiLU}(\mathbf{z})
15: \mathbf{H}_l: (B, L, D) \leftarrow \text{Linear}^{\mathbf{H}}(y'_{\text{forward}} + y'_{\text{backward}}) + \mathbf{H}_{l-1}
 16: return \mathbf{H}_l
```

Algorithm 2 ExtBiMamba Layer Workflow

```
Require: \mathbf{H}_{l-1}: (B, L, D)
Ensure: \mathbf{H}_l: (B, L, D)
   1: \mathbf{H}'_{l-1}: (B, L, D) \leftarrow \mathbf{Norm}(\mathbf{H}_{l-1})
  2: for o \in \{\text{forward}, \text{backward}\}\ do
                \mathbf{x}_o: (\mathsf{B}, \mathsf{L}, \mathsf{E}) \leftarrow \mathbf{Linear}_o^{\mathbf{x}}(\mathbf{H}_{l-1}')
                \mathbf{z}_o: (\mathsf{B}, \mathsf{L}, \mathsf{E}) \leftarrow \mathbf{Linear}_o^{\mathbf{z}}(\mathbf{H}_{l-1}')
   4:
                \mathbf{x}_o': (B, L, E) \leftarrow SiLU(Conv1d_o(\mathbf{x}_o))
               \mathbf{B}_o: (\mathtt{B}, \mathtt{L}, \mathtt{N}) \leftarrow \mathbf{Linear}_o^{\mathbf{B}}(\mathbf{x}_o')
                \mathbf{C}_o : (\mathsf{B}, \mathsf{L}, \mathsf{N}) \leftarrow \mathbf{Linear}_o^{\mathbf{C}}(\mathbf{x}_o')
                \Delta_o: (B,L,E) \leftarrow \log(1 + \exp(\operatorname{Linear}_o^{\Delta}(\mathbf{x}_o') +
                \mathbf{Parameter}_{o}^{\Delta}))
                \overline{\mathbf{A}}_o: (\mathsf{B}, \mathsf{L}, \mathsf{E}, \mathsf{N}) \leftarrow \mathbf{\Delta}_o \otimes \mathbf{Parameter}_o^{\mathbf{A}}
  9:
                \overline{\mathbf{B}}_o: (B, L, E, N) \leftarrow \Delta_o \bigotimes \mathbf{B}_o
 10:
               \mathbf{y}_{o}: (\texttt{B}, \texttt{L}, \texttt{E}) \leftarrow \mathbf{SSM}\left(\overline{\mathbf{A}}_{o}, \overline{\mathbf{B}}_{o}, \mathbf{C}_{o}\right)(\mathbf{x}_{o}')
\mathbf{y}_{o}': (\texttt{B}, \texttt{L}, \texttt{D}) \leftarrow \mathbf{Linear}_{o}^{\mathbf{H}}(\mathbf{y}_{o} \odot \mathbf{SiLU}(\mathbf{z}_{o}))
 11:
 12:
 13: end for
 14: \mathbf{H}_l: (B, L, D) \leftarrow (y'_{\text{forward}} + y'_{\text{backward}}) + \mathbf{H}_{l-1}
 15: return H_l
```

Algorithms 1 and 2 illustrate the workflows of InnBiMamba and ExtBiMamba, respectively. The main differences are highlighted in violet. For the InnBiMamba layer, the linear input projections (**Linear**^x and **Linear**^z) and the linear output projection **Linear**^H are shared across forward and backward operations. In contrast, the ExtBiMamba layer uses different input linear projections (**Linear**^x_o and **Linear**^z_o) and output linear projections (**Linear**^H_o) across forward and backward operations.

IV. EXPERIMENTAL SETUP

A. Speech Enhancement

Datasets. We follow previous works [29], [30] and employ the clean speech data from the LibriSpeech train-clean-100 corpus [31] as the training set, containing 28 539 speech clips spoken by 251 speakers. The noise recordings are collected from the following datasets [32], i.e., the noise data of the MUSAN datasets [33], the RSG-10 dataset [34] (voice babble, F16, and factory welding are excluded for testing), the Environmental Noise dataset [35], [36], the colored noise set (with an α value ranging from -2 to 2 in increments of 0.25) [37], the UrbanSound dataset [38] (street music recording no 26 270 is excluded for testing), the QUT-NOISE dataset [39], and the Nonspeech dataset [40].

Noise recordings that exceeds 30 seconds in duration are split into clips of 30 seconds or less. This yields 6 809 noise clips, with each clip less than or equal to 30 seconds in duration. For validation experiments, 1 000 clean speech and noise clips (without replacement) were randomly drawn from the aforementioned clean speech and noise sets and mixed to generate a validation set of 1 000 noisy clips, where each clean speech clip was degraded by a random section of one noise clip at a random SNR level (sampled between -10 and 20 dB, in 1 dB steps). For evaluation experiments, we employed four real-world noise sources (excluded from the training set) including two non-stationary and two colored ones.

The two non-stationary noise sources were the *voice babble* from the RSG-10 noise dataset [34] and *street music* from the Urban Sound dataset [38]. The two colored noise sources were *F16* and *factory welding* from RSG-10 noise dataset [34]. For each of the four noises, we randomly picked twenty clean speech clips (without replacement) from the *test-clean-100* of LibriSpeech corpus [31] and degraded each clip with a random section of the noise clip at the five SNR levels, i.e., $\{-5 \text{ dB}, 0 \text{ dB}, 5 \text{ dB}, 10 \text{ dB}, 15 \text{ dB}\}$. This generated 400 noisy mixtures for evaluation.

Feature Extraction. All audio signals are sampled at a rate of 16 kHz. We employ a 512-sample (32 ms) long square-root-Hann window with a hop length of 256 samples (16 ms), to extract a 257-point single-sided STFT spectral magnitude as the input to the neural models [32].

Model Configurations. In our experiments, we employ the same backbone network architecture (a typical neural solution to speech enhancement) [32], [30], [41], [42], which comprises an input embedding layer, stacked feature transformation layers (such as Mamba, Transformer, and Conformer layers), and an output layer. To systematically study the Mamba networks, we use the standard Transformer [32], [30] and Conformer [9] models as the baseline backbone networks, across causal and non-causal configurations.

To perform extensive comparison studies across different model sizes, we use the Transformer and Conformer architectures comprising $N \in \{4, 6\}$ stacked Transformer and Conformer layers respectively [32]. For the Transformer speech enhancement backbone, we follow the configuration in [30], [32]: the layer dimension $d_{\text{model}} = 256$, the number of attention heads H = 8, and the inner-layer size of the feed-forward network (FFN) $d_{ff} = 1024$. For the Conformer backbone, we adopt the parameter configurations in [32]: the layer dimension $d_{\text{model}} = 256$, the number of attention heads H = 8, the kernel size of convolution 32, the expansion factor for convolution module 2, and the inner-layer size of FFN $d_{ff} = 1024$. For the Mamba model, we use the parameter configurations in [16]: the model dimension D=256, the SSM state dimension N=16, the local convolution width $d_{conv} = 4$, and the expansion factor E=2. All the experiments were run on an NVIDIA Tesla V100-SXM2-32GB GPU.

Training strategy. We use mean-square error (MSE) on the power-law compressed spectral magnitude as the objective loss function [43]. The noisy mixtures are dynamically generated at training time. For each minibatch, we randomly pick 10 clean speech clips and degraded each clip by a random section of a random noise clip at a random SNR level sampled from -10 to 20 dB (in 1 dB steps). The Adam optimization algorithm [44] is employed for gradient descent, with parameters as in [1], i.e., $\beta_1 = 0.9$, $\beta_2 = 0.98$, and $\epsilon = 10^{-9}$. We utilize the gradient clipping technology to cut the gradient values to a range between -1 and 1. All the models are trained for 150 epochs for fair comparison. The warm-up strategy is adopted to adjust the learning rate: $lr = d_{model}^{-0.5} \cdot \min(n_step^{-0.5}, n_step \cdot w_steps^{-1.5}), \text{ where}$ n_step and w_steps denote the iteration steps and the warmup iteration steps, respectively. We follow the study [32] and set w_steps as 40000.

TABLE I: Implementation details in different tasks and datasets. We show the best Transformer configurations reported in ESPnet Official

	LibriSpeech100	LibriSpeech960	ASRU	SEAME
Frontend				
window length	400	400	400	400
hop length	160	128	160	160
SpecAug				
time warp window	5	5	5	5
num of freq masks	2	2	2	2
freq mask width	(0, 27)	(0, 30)	(0, 27)	(0, 27)
num of time masks	2	2	2	2
time mask width	(0, 0.05)	(0, 40)	(0, 0.05)	(0, 0.05)
Architecture				
feature size d	256	512	256	256
hidden size d_{hidden}	1024	2048	1024	2048
attention heads h	4	8	4	4
num of encoder layers	18	18	18	24
depth-wise conv kernel	31	31	31	31
Training				
epochs	70	100	70	70
learning rate	2e-3	2e-3	2e-3	2e-3
warmup steps	15k	25k	15k	15k
weight decay	1e-6	1e-6	1e-6	1e-6
dropout rate	0.1	0.1	0.1	0.1
ctc weight	0.3	0.3	0.3	0.3
label smoothing	0.1	0.1	0.1	0.1

TABLE II: Implementation details in different tasks and datasets. We show the best Conformer configurations reported in ESPnet Official

	LibriSpeech100	LibriSpeech960	ASRU	SEAME
Frontend	Libriopecciiroo	Dioriopeccinous	715ItC	SERVIE
window length	400	400	400	400
hop length	160	160	160	160
SpecAug	100	100	100	100
time warp window	5	5	5	5
num of freq masks	2	2	2	2
freq mask width	(0, 27)	(0, 27)	(0, 30)	(0, 30)
num of time masks	2	2	2	(0, 30)
time mask width	(0, 0.05)	(0, 0.05)	(0, 40)	(0, 40)
Architecture				
feature size d	256	512	256	256
hidden size dhidden	1024	2048	2048	2048
attention heads h	4	8	4	4
num of encoder layers	12	12	12	12
depth-wise conv kernel	31	31	31	31
Training				
epochs	120	50	70	70
learning rate	2e-3	2.5e-3	1e-3	1e-3
warmup steps	15k	40k	25k	25k
weight decay	1e-6	1e-6	1e-6	1e-6
dropout rate	0.1	0.1	0.1	0.1
ctc weight	0.3	0.3	0.3	0.3
label smoothing	0.1	0.1	0.1	0.1

Evaluation Metrics. We evaluate enhanced speech with five commonly used assessment metrics, i.e, perceptual evaluation of speech quality (PESQ) [45], extended short-time objective intelligibility (ESTOI), and three composite metrics. For PESQ, both wide- and narrow-band PSEQ were used to evaluate the speech quality, with the score range of [-0.5, 4.5]. The ESTOI [46] score is typically between 0 and 1. The three composite metrics [47] are used to predict the mean opinion scores of the intrusiveness of background noise (CBAK), the signal distortion (CSIG), and the overall signal quality (COVL), respectively, with the score range of [0, 5]. For all these five metrics, a higher score means better performance.

TABLE III: Implementation details in different tasks and datasets. We show the best branchformer configurations reported in ESPnet Official

	LibriSpeech100	LibriSpeech960	ASRU	SEAME
Frontend				
window length	400	400	400	400
hop length	160	160	160	160
SpecAug				
time warp window	5	5	5	5
num of freq masks	2	2	2	2
freq mask width	(0, 27)	(0, 27)	(0, 27)	(0, 27)
num of time masks	2	2	2	2
time mask width	(0, 0.05)	(0, 0.05)	(0, 0.05)	(0, 0.05)
Architecture				
feature size d	256	512	256	256
hidden size d_{hidden}	1024	2048	2048	1024
attention heads h	4	8	4	4
num of encoder layers	12	18	12	12
depth-wise conv kernel	31	31	31	31
Training				
epochs	70	70	70	70
learning rate	2e-3	2.5e-3	2e-3	2e-3
warmup steps	15k	40k	15k	15k
weight decay	1e-6	1e-6	1e-6	1e-6
dropout rate	0.1	0.1	0.1	0.1
ctc weight	0.3	0.3	0.3	0.3
label smoothing	0.1	0.1	0.1	0.1

B. Speech Recognition

Datasets. We evaluate our models on ASR with four datasets, i.e., LibriSpeech [31], AN4 [48], SEAME [49], and ASRU [50], in which all speech signals are sampled at 16 kHz. LibriSpeech (LibriSpeech960) containing approximately 1000 hours of audio recordings and their paired texts, in which a subset LibriSpeech100 is used for ablation studies due to its higher recording quality. The AN4 dataset contains approximately one hour of audio recordings of primarily spoken alphanumeric strings, such as postal codes and telephone numbers. It is employed to assess the model's ability to perform with a small dataset. Two English-Mandarin code-switching datasets SEAME and ASRU-CS-2019 (denoted as ASRU) are then used for a more challenging scenario compared to monolingual. The SEAME dataset contains 200-hour spontaneous South-east Asian-accented speech with intra- and inter-sentential codeswitches, divided as introduced in [51]. The ASRU dataset contains a 500-hour Mandarin and a 200-hour code-switching training sets recorded in mainland China, where only the codeswitching set is used for training, following [49], [50], [52].

For Mamba and BiMamba models, we employ the default hyper-parameters [16]: the state dimension $d_{\rm state}\!=\!16$, convolution dimension $d_{\rm conv}\!=\!4$, and the expansion factor was set to 2. To keep the same batch size as in the official implementation of ESPnet, the experiments on the LibriSpeech-960 dataset were performed on an NVIDIA A100 80GB. All the other experiments were run on an NVIDIA V100 32GB.

The detailed model configurations for each dataset are given in Tables I, II and III.

Evaluation Metrics. We employ word error rate (WER) and mixed word error rate (MER) to measure the ASR performance for monolingual and code-switching ASR tasks, respectively, where the MER considers the word error rate for English and the character error rate for Mandarin. All experiments are performed using the ESPnet toolkit [53]

TABLE IV: Comparison results of InnBiMamba and ExtBi-Mamba architectures in NB-PESQ, WB-PESQ, ESTOI (%), CSIG, CBAK, and COVL. The BiMamba models are denoted as "Inn/ExtBiMamba-the number of BiMamba layers".

Method	#Params	Causality		Metrics				
			NB-PESQ	WB-PESQ	ESTOI	CSIG	CBAK	COVL
Noisy	-	_	1.88	1.24	56.12	2.26	1.80	1.67
InnBiMamba-9	4.48 M	X	2.84	2.14	75.74	3.39	2.59	2.74
ExtBiMamba-5	4.51 M	×	2.86	2.15	76.12	3.46	2.60	2.78
InnBiMamba-13	6.41 M	_ ×	2.90	2.19	76.89	3.50	2.63	2.82
ExtBiMamba-7	6.26 M	X	2.90	2.20	77.04	3.54	2.64	2.84

TABLE V: Evaluation results of InnBiMamba and ExtBiMamba in training speed (training time per step) and inference speed (RTF).

	InnBiMamba-9	ExtBiMamba-5	InnBiMamba-13	ExtBiMamba-7
sec/step	0.159		0.212	0.159
RTF	1.88×10^{-4}	1.69×10^{-4}	2.76×10^{-4}	2.34×10^{-4}

V. EXPERIMENTAL RESULTS AND ANALYSIS

A. Speech Enhancement

InnBiMamba vs. ExtBiMamba. In Table IV, we illustrate the comparison results of InnBiMamba and ExtBiMamba across different model sizes, in terms of six metrics, i.e., NB-PESQ, WB-PESQ, ESTOI, CSIG, CBAK, and COVL. Overall, ExtBiMamba consistently performs slightly better than InnBiMamba across the model sizes. In addition, Table V compares the training speed (training time per step) and inference speed (real-time factor [54]) of InnBiMamba and ExtBiMamba, confirming the superiority of ExtBiMamba over InnBiMamba. Real-time factor (RTF) is measured by dividing the time taken to process a speech utterance by the duration of the speech. The RTFs were measured on an NVIDIA Tesla V100 GPU and averaged over 20 executions. We use a batch size of 4 noisy mixtures, each with a duration of 10 seconds [54].

Mamba vs. Transformer. Table VI compares Transformer and Mamba network architectures. For Mamba models, we report the results of Mamba models with the same number of layers and a similar model size to the Transformer. It can be observed that the Mamba models consistently demonstrate obvious performance superiority over the Transformer models with lower parameter overheads, across causal and noncausal configurations. For instance, the Mamba-7 (3.20 M) and ExtBiMamba-5 (4.51 M) improve on the causal Transformer-4 (3.29 M) and the noncausal Transformer-6 (4.81 M) by 0.08 and 0.08, 0.07 and 0.1, 2.14% and 1.56%, 0.09 and 0.08, 0.06 and 0.08, and 0.09 and 0.09 in terms of NB-PESQ, WB-PESQ, ESTOI, CSIG, CBAK, and COVL, respectively. In addition, ExtBiMamba models provide substantial performance improvements over original (unidirectional) Mamba models across all the metrics, which confirms the effectiveness of the bidirectional modeling. ExtBiMamba-5 (4.51 M) provided gains of 0.18 in NB-PESQ, 0.21 in WB-PESQ, 2.92% in ESTOI, 0.16 in CSIG, 0.13 in CBAK, and 0.19 in COVL over Mamba-10 (4.51 M), respectively. Table VII presents the comparison results of Mamba and Transformers in training

TABLE VI: Performance comparisons of Transformer and Mamba network architectures in NB-PESQ, WB-PESQ, ESTOI (%), CSIG, CBAK, and COVL, across causal and non-causal configurations. Transformers with 4 and 6 stacked Transformer layers are denoted as Transformer-4 and Transformer-6, respectively.

Method	#Params	Causality	Metrics					
			NB-PESQ	WB-PESQ	ESTOI	CSIG	CBAK	COVL
Noisy	_	-	1.88	1.24	56.12	2.26	1.80	1.67
Transformer-4	3.29 M	~	2.56	1.84	70.32	3.17	2.39	2.47
Mamba-4	1.88 M	~	2.60	1.87	70.99	3.17	2.41	2.48
Mamba-7	3.20 M	~	2.64	1.91	72.46	3.26	2.45	2.56
Transformer-4	3.29 M	x	2.74	2.01	73.44	3.31	2.50	2.63
ExtBiMamba-3	2.76 M	X	2.76	2.05	73.93	3.36	2.53	2.67
ExtBiMamba-4	3.64 M	X	2.83	2.11	75.43	3.46	2.57	2.75
Transformer-6	4.86 M	x _	2.78	2.05	74.56	3.38	2.52	2.69
ExtBiMamba-5	4.51 M	X	2.86	2.15	76.12	3.46	2.60	2.78
ExtBiMamba-6	5.39 M	Х	2.88	2.17	76.69	3.50	2.62	2.82

TABLE VII: Training speed and inference speed of ExtBi-Mamba and non-causal Transformers.

					ExtBiMamba-6	
sec/step	0.099	0.089	0.102	0.125	0.122	0.141
RTF(10s)	1.48×10^{-4}	1.08×10^{-4}	1.38×10^{-4}	2.12×10^{-4}	1.71×10^{-4}	2.04×10^{-4}
RTF(40s)	3.94×10^{-4}	6.95×10^{-5}	9.14×10^{-5}	5.89×10^{-4}	1.13×10^{-4}	$0.141 \\ 2.04 \times 10^{-4} \\ 1.35 \times 10^{-4}$

speed and inference speed (10s and 40s inference lengths), confirming the obvious its superiority over Transformer in inference speed, especially for longer inference length.

Mamba vs. Conformer. Table VIII reports the comparative results of Conformer and Mamba. We can see that original Mamba (causal) models outperform causal Conformer models across all metrics while involving fewer parameters. For instance, compared to causal Conformer-6 (9.26 M), Mamba-20 (8.89 M) improves NB-PESQ by 0.04, WB-PESQ by 0.06, ESTOI by 0.68%, CSIG by 0.05, CBAK by 0.05, and COVL by 0.06. It can also be seen that overall, ExtBiMamba models exhibit slightly better or comparable performance to noncausal Conformer models. The substantial performance superiority of the bidirectional modeling is observed from evaluation results of ExtBiMamba-6 (5.39 M) vs. Mamba-13 (5.83M) and ExtBiMamba-10 (8.89 M) vs. Mamba-20 (8.89 M).

Mamba vs. MHSA. We also explore replacing the MHSA with the Mamba layer in Transformer and Conformer. Tables X-XI present the evaluation results of replacing the MHSA module in Transformer and Conformer with the Mamba layer. It can be observed that Transformers substantially benefit from using the Mamba and BiMamba layers. TransMamba-4 and TransExtBiMamba-6 improve over causal Transformer-4 and non-causal Transformer-6 by 0.09 and 0.13 in NB-PESQ, 0.09 and 0.16 in WB-PESQ, 1.96% and 4.04% in ESTOI, 0.07 and 0.22 in CSIG, 0.06 and 0.13 in CBAK, and 0.08 and 0.19 in COVL, respectively. In addition, TransMamba-4 (3.99 M) and TransInnBiMamba-4 (4.17 M) outperform causal Transformer-6 (4.86 M) and non-causal Transformer (4.86 M), respectively, which further confirms the superiority of Mamba layer over MHSA. Among InnBiMamba and ExtBiMamba, we observe that TransExtBiMamba performs slightly better than TransInnBiMamba. With fewer parameters, TransExtBiMamba-

TABLE VIII: Speech enhancement performance comparisons of Conformer and Mamba network architectures in NB-PESQ, WB-PESQ, ESTOI (%), CSIG, CBAK, and COVL, across causal and noncausal configurations. The Conformer models with 4 and 6 Conformer layers are denoted as Conformer-4 and Conformer-6, respectively.

Method	#Params	Causality		Metrics					
			NB-PESQ	WB-PESQ	ESTOI	CSIG	CBAK	COVL	
Noisy	-	_	1.88	1.24	56.12	2.26	1.80	1.67	
Conformer-4	6.22 M	~	2.67	1.94	72.78	3.30	2.46	2.59	
Mamba-13	5.83 M	~	2.70	1.97	73.53	3.32	2.50	2.62	
Conformer-4	6.22 M	_ x	2.88	2.17	76.68	3.51	2.61	2.82	
ExtBiMamba-6	5.39 M	X	2.88	2.18	76.73	3.50	2.62	2.82	
ExtBiMamba-7	6.26 M	Х	2.90	2.20	77.04	3.54	2.64	2.84	
Conformer-6	9.26 M	~	2.68	1.94	73.41	3.30	2.46	2.59	
Mamba-20	8.89 M	~	2.72	2.00	74.09	3.35	2.51	2.65	
Conformer-6	9.26 M	_ x _	2.91	2.20	77.56	3.54	2.62	2.84	
ExtBiMamba-10	8.89 M	X	2.91	2.20	77.64	3.59	2.65	2.87	

TABLE IX: Training speed and inference speed of ExtBiMamba and non-causal Conformers.

	Conformer-4	ExtBiMamba-6	ExtBiMamba-7	Conformer-6	ExtBiMamba-10
sec/step	0.160	0.142	0.156	0.215	0.206
RTF	2.27×10^{-4}	2.07×10^{-4}	2.37×10^{-4}	3.27×10^{-4}	3.32×10^{-4}

4 (5.74 M) achieves slightly higher scores in WB-PESQ, CSIG, CBAK, and COVL, but slightly lower scores in NB-PESQ and ESTOI than TransInnBiMamba-6 (6.19 M).

As shown in Table XI, we observe that the Conformer architecture can benefit from the use of Mamba and ExtBi-Mamba. The ConExtBiMamba-4 and ConExtBiMamba-6 outperform non-causal Conformer-4 and Conformer-6 by 0.04 and 0.02 in NB-PESQ, 0.03 and 0.03 in WB-PESQ, 1.06% and 0.65% in ESTOI, 0.06 and 0.06 in CSIG, 0.03 and 0.03 in CBAK, and 0.06 and 0.05 in COVL, respectively. In addition, ConExtBiMamba-4 (8.67 M) also exhibits a slightly better performance than non-causal Conformer-6 (9.26 M). Among InnBiMamba and ExtBiMamba, similarly, ConExtBiMamba performs better than ConvInnBiMamba.

B. Speech Recognition

Independent vs. Substitute for MHSA. Table XIII reports the performance of Mamba when used independently and as a replacement for MHSA across various datasets. We can observe that independent Mamba and BiMamba models exhibit significantly lower performance compared to the Transformer and Conformer models (with the same number of layers). Since the Mamba has fewer parameters when configured with the same number of layers as the Transformer and Conformer, we increased its number of layers as shown in Table XIV to match the number of parameters with the Conformer to further evaluate Mamba for ASR. The performance of Mamba, however, remained undesirable. In contrast to the independent Mamba/BiMamba, we observe a significant improvement in the ASR task when Mamba/BiMamba is used as a replacement for MHSA. Specifically, replacing MHSA with ExtBiMamba in the Conformer (named ConExtBiMamba) exhibits higher performance than the SOTA performance achieved by Con-

TABLE X: Evaluation results for replacing the MHSA with Mamba/BiMamba layer in Transformer network, across causal and noncausal configurations.

#Params	Causality	Metrics					
		NB-PESQ	WB-PESQ	ESTOI	CSIG	CBAK	COVL
-	-	1.88	1.24	56.12	2.26	1.80	1.67
3.29 M	~	2.56	1.84	70.32	3.17	2.39	2.47
3.99 M	~	2.65	1.93	72.28	3.24	2.45	2.55
3.29 M	_ x	2.74	2.01	73.44	3.31	2.50	2.63
4.17 M	X	2.86	2.15	76.24	3.44	2.61	2.78
5.74 M	X	2.88	2.18	76.75	3.54	2.63	2.84
4.86 M	~	2.60	1.87	71.37	3.20	2.41	2.50
5.92 M	~	2.68	1.95	73.04	3.31	2.48	2.60
4.86 M	x	2.78	2.05	74.56	3.38	2.52	2.69
6.19 M	X	2.89	2.17	77.22	3.49	2.61	2.80
8.54 M	X	2.91	2.21	77.60	3.60	2.65	2.88
	3.29 M 3.99 M 3.29 M 4.17 M 5.74 M 4.86 M 5.92 M 4.86 M 6.19 M	3.29 M	1.88 3.29 M	NB-PESQ WB-PESQ -	NB-PESQ WB-PESQ ESTOI - - 1.88 1.24 56.12 3.29 M ✓ 2.56 1.84 70.32 3.29 M ✓ 2.65 1.93 72.28 3.29 M X 2.74 2.01 73.44 4.17 M X 2.86 2.15 76.24 5.74 M X 2.88 2.18 76.75 4.86 M ✓ 2.60 1.87 71.37 5.92 M ✓ 2.68 1.95 73.04 4.86 M X 2.78 2.05 74.56 6.19 M X 2.89 2.17 77.22	NB-PESQ WB-PESQ ESTOI CSIG - - 1.88 1.24 56.12 2.26 3.29 M ✓ 2.56 1.84 70.32 3.17 3.99 M ✓ 2.65 1.93 72.28 3.24 3.29 M X 2.74 2.01 73.44 3.31 4.17 M X 2.86 2.15 76.24 3.44 5.74 M X 2.88 2.18 76.75 3.54 4.86 M ✓ 2.60 1.87 71.37 3.20 5.92 M ✓ 2.68 1.95 73.04 3.31 4.86 M X 2.78 2.05 74.56 3.38 6.19 M X 2.89 2.17 77.22 3.49	NB-PESQ WB-PESQ ESTOI CSIG CBAK - - 1.88 1.24 56.12 2.26 1.80 3.29 M ✓ 2.56 1.84 70.32 3.17 2.39 3.99 M ✓ 2.65 1.93 72.28 3.24 2.45 3.29 M X 2.74 2.01 73.44 3.31 2.50 4.17 M X 2.86 2.15 76.24 3.44 2.61 5.74 M X 2.88 2.18 76.75 3.54 2.63 4.86 M ✓ 2.60 1.87 71.37 3.20 2.41 5.92 M ✓ 2.68 1.95 73.04 3.31 2.48 4.86 M X 2.78 2.05 74.56 3.38 2.52 6.19 M X 2.89 2.17 77.22 3.49 2.61

TABLE XI: Evaluation results for replacing the MHSA with Mamba/BiMamba layer in Conformer network, across causal and noncausal configurations.

Method	#Params Causality		Metrics					
			NB-PESQ	WB-PESQ	ESTOI	CSIG	CBAK	COVI
Noisy	-	_	1.88	1.24	56.12	2.26	1.80	1.67
Conformer-4	6.22 M	~	2.67	1.94	72.78	3.29	2.45	2.58
- MHSA + Mamba	6.92 M	~	2.69	1.95	73.27	3.29	2.48	2.59
Conformer-4	6.22 M	_ x	2.88	2.17	76.68	3.51	2.61	2.82
- MHSA + InnBiMamba	7.10 M	×	2.89	2.17	77.40	3.51	2.62	2.81
- MHSA + ExtBiMamba	8.67 M	Х	2.92	2.20	77.74	3.57	2.64	2.88
Conformer-6	9.26 M	~	2.68	1.94	73.41	3.30	2.46	2.59
- MHSA + Mamba	10.32 M	~	2.71	1.95	73.69	3.34	2.49	2.62
Conformer-6	9.26 M	_ x	2.91	2.20	77.56	3.54	2.62	2.84
- MHSA + InnBiMamba	10.59 M	×	2.92	2.19	77.85	3.52	2.64	2.83
- MHSA + ExtBiMamba	12.94 M	Х	2.93	2.23	78.21	3.60	2.65	2.89

TABLE XII: Training speed and inference speed of Transformer and TranBiMamba, and Conformer and ConBiMamba.

	Transformer-6	TransInnBiMamba-6	TransExtBiMamba-6	Conformer-6	ConInnBiMamba-6	ConExtBiMamba-6
sec/step	0.125	0.155	0.161	0.215	0.206	0.214
RTF	2.12×10^{-4}	1.81×10^{-4}	1.95×10^{-4}	3.27×10^{-4}	2.85×10^{-4}	2.99×10^{-4}

former and Branchformer across multiple datasets with the same training setups. Additionally, ConExtBiMamba provides faster training and inference speeds compared to the Conformer model as detailed in Table XVII. When we replaced MHSA with ExtBiMamba, the number of parameters exceeded that of the original Conformer. To eliminate the possibility that the performance improvement results from the higher number of parameters, we increase the size of Conformer to a similar number of parameters as ConExtBiMamba, and present the results in Table XV. We found that although the Conformer's performance improves, it still underperforms ConExtBiMamba and ConInnBiMamba, supporting the effectiveness of our approach.

Unidirectional vs. Bidirectional. Tables XIII-XV present the evaluation results of unidirectional Mamba and two bidirectional Mamba modules (InnBiMamba and ExtBiMamba) along with their model sizes. Both InnBiMamba and ExtBiMamba show significant improvements over unidirectional Mamba when replacing the MHSA module in Transformer and Conformer frameworks, confirming the effectiveness of bidirectional modeling.

Additionally, ExtBiMamba consistently outperforms InnBi-

TABLE XIII: ASR results for the different datasets without language model in WER/MER (%). "ESPnet" means the best result reported by ESPnet official or other paper experimented with ESPnet, where the SEAME and ASRU results come from [55], [56], [52].

Method	LibriS	peech-10	00 LibriS	peech-96	0 SEA	ME	AS	RU
	dev	test	dev	test	man	sge	dev	test
ESPnet								
Conformer	6.3	6.5	2.1	2.4	16.6	23.3	-	12.2
Branchformer	6.1	6.3	2.2	2.4	-	-	-	-
Reproduced Results								
Branchformer	6.3	6.4	2.2	2.4	16.3	23.2	12.5	11.8
Mamba	40.8	40	21.8	22.3	44.5	55.3	38.0	36.3
InnBiMamba	39.6	38.2	21.8	22.5	44.3	55.4	38.4	37.9
ExtBiMamba	38.5	37.7	21.6	22.1	44.4	55.2	38.2	36.8
Transformer	8.0	8.4	2.8	3.2	17.7	24.5	13.7	13.1
- MHSA $+$ Mamba	10.9	11.2	3.2	3.5	20.7	29.5	24.2	23.1
- MHSA + InnBiMamba	8.8	9.4	2.5	3.0	18.4	26.0	20.2	19.5
- MHSA + ExtBiMamba	8.4	8.7	2.5	2.8	17.2	24.3	18.7	18.0
Conformer	6.3	6.5	2.3	2.6	16.9	23.6	12.8	12.2
- MHSA $+$ Mamba	6.6	6.9	2.6	2.9	17.7	24.9	13.5	12.9
- MHSA $+$ InnBiMamba	6.0	6.4	2.1	2.3	17.1	23.8	12.7	12.2
- MHSA + ExtBiMamba	5.9	6.0	2.0	2.3	16.6	23.4	12.3	11.5

TABLE XIV: WER/MER results (%) for LibriSpeech100 and SEAME: the left part displays results from LibriSpeech100, while the right part shows results from SEAME.

Method	#Params (M	l) dev	test	#Params (M) man	sge
Conformer	34.23	6.3	6.5	47.27	16.9	23.6
Transformer	29.38	8.0	8.4	29.38	17.7	24.5
Mamba-based Mod	els			1		
Mamba	20.41	40.8	40	20.41	44.5	55.3
Mamba Large	32.52	38.8	39.2	28.78	45.5	55
ExtBiMamba	25.79	38.5	37.7	25.79	44.4	55.2
ExtBiMamba Large	33.52	37.8	37.2	33.52	43.6	54.3

Mamba across various frameworks and datasets, as demonstrated in Tables XV and XVI. Even when increasing the number of layers in InnBiMamba to match the parameter count of ExtBiMamba for a fair comparison, ExtBiMamba still achieves better performance. Moreover, further comparisons with Conformer-Large and ConInnBiMamba-Large indicate that the performance improvements in ASR are not solely due to an increase in model parameters.

C. Ablation Study on ConExtBiMamba

We employ the ConExtBiMamba model, which improves the SOTA result achieved by Branchformer in the ASR task, for ablation studies.

Hyper-Parameter for BiMamba in ConExtBiMamba. The default hyper-parameters for ConExtBiMamba are defined as: the SSM state dimension $d_{\rm state}=16$, the state expansion factor E=2, and the local convolution width $d_{\rm conv}=4$. From Table XVIII, we find that increasing the state expansion factor or decreasing the local convolution width has little impact on the performance of ConExtBiMamba.

We further investigate the impact of the A matrix on performance. The A matrix plays a crucial role in both S4 and

TABLE XV: WER results on LibriSpeech (without external language model) across various parameter counts and frameworks.

Method	Params (M)	dev	dev other	test	test other
LibriSpeech100					
Transformer	29.38	8.0	20.0	8.4	20.2
- MHSA + InnBiMamba	33.32	8.8	23.3	9.4	23.6
- MHSA + ExtBiMamba	40.42	8.4	22.4	8.7	23.1
Conformer Large	42.17	6.2	17.4	6.4	17.3
Conformer	34.23	6.3	17.4	6.5	17.3
- MHSA + InnBiMamba	36.89	6.0	17.4	6.4	17.6
- MHSA + InnBiMamba Large	49.90	6.1	17.3	6.3	17.3
- MHSA + ExtBiMamba	41.59	5.9	17.1	6.0	17.2
LibriSpeech960					
Transformer	99.36	2.8	7.6	3.2	7.5
- MHSA + InnBiMamba	103.35	2.5	7.4	3.0	7.3
- MHSA + ExtBiMamba	110.04	2.5	6.9	2.8	6.9
Conformer	116.15	2.3	5.5	2.6	5.6
- MHSA + InnBiMamba	118.81	2.1	5.6	2.4	5.5
- MHSA + ExtBiMamba	123.51	2.0	5.4	2.3	5.4

TABLE XVI: InnBiMamba vs. ExtBiMamba: MER Results (%) on ASRU and SEAME. Left results are from ASRU, right results are from SEAME.

Method	Params (M)	dev	test	Params (M)	man	sge
Transformer	30.86	13.7	13.1	29.86	17.7	24.5
 MHSA + InnBiMamba 	34.80	20.2	19.5	33.81	18.4	26.0
– MHSA + ExtBiMamba	44.24	18.7	18	43.25	17.2	24.3
Conformer	48.27	$1\overline{2.8}$	12.2	- _{47.27} -	16.9	$2\overline{3}.6$
 MHSA + InnBiMamba 	50.10	12.7	12.2	49.11	17.1	23.8
– MHSA + ExtBiMamba	56.40	12.3	11.5	55.40	16.6	23.4

TABLE XVII: Training speed (mins/epoch) and Inference speed (RTF) for ASR in LibriSpeech100 on NVIDIA Tesla V100.

	Conformer	ConInnBiMamba	ConExtBiMamba
mins/epoch	21.4	18.3	19.8
RTF	0.179	0.174	0.177

Mamba. In the original Mamba paper, it is initialized using a real-valued diagonal matrix. However, ensuring randomness is important in deep learning [57]. To explore this, we examine three types of A matrices: a real-valued diagonal matrix, a completely randomized matrix, and a real-valued diagonal matrix initialized by multiplying each element with noise generated from a Gaussian distribution. Through our experiments, we discovered that the diagonal matrix with Gaussian noise yielded the best results.

Hyper-Parameters for ConExtBiMamba We conduct ablation experiments on Swish Activation, Macaron-style feed-forward layers, positional encoding, and dropout. From Table XIX, it is apparent that Swish Activation and Macaron-style feed-forward layers enhance the model's performance, while positional encoding and dropout do not have a significant impact. We suggest that the reason positional encoding, a crucial component in Transformer-based models, does not significantly affect the ConExtBiMamba model is twofold. Firstly, Mamba independently models each input, which suggests that the model may better differentiate between different positions. Secondly, because Mamba operates similarly to an RNN, the

TABLE XVIII: Ablation Study on LibriSpeech100 for ConExtBiMamba by employing WER (%)

Method	dev (↓) d	lev other (↓	.) test (\bigcup)	test other (\dagger)
ConvExtBiMamba with Gaussian Noise	5.9	17.1	6.0	17.3
$\rightarrow d_{\mathrm{state}} = 32$	5.9	17.1	6.0	17.3
$\rightarrow d_{\rm conv} = 2$	6.0	17.1	6.2	17.3
$\rightarrow E = 4$	5.9	17.1	6.0	17.3
→ Random Noise A matrix	6.0	17.2	6.2	17.4
→ default A matrix	6.1	17.2	6.2	17.5

TABLE XIX: Ablation Studies for ConExtBiMamba on LibriSpeech100.

Method	dev (↓) d	dev other (\d	test (\dagger) t	est other (\psi)
ConExtBiMamba	5.9	17.1	6.0	17.3
Macaron	6.1	17.7	6.3	17.9
- Swish	6.2	17.7	6.4	18.1
Dropout	6.0	17.1	6.0	17.4
+ Positional Encoding	6.0	17.1	6.0	17.3

dependencies between inputs inherently embed some positional information into the model, thus diminishing the impact of positional encoding.

Performance on Extremely Small Datasets To evaluate model robustness, we conduct tests on the AN4 dataset—a notably small dataset—using five randomly selected seeds for both the Conformer and ConExtBiMamba models under identical hyperparameters. Our results show that ConExtBi-Mamba consistently outperforms the Conformer across all seeds. Specifically, the mean WER for the Conformer was 10.02, while it was significantly lower for ConExtBiMamba at just 4.54. Remarkably, ConExtBiMamba also demonstrated exceptional robustness, with a WER variance of only 1.11 compared to the Conformer's substantially higher variance of 77.71. Observing the loss metrics, we noted that ConBiMamba is less prone to overfitting on small datasets compared with the Conformer. This suggests that ConBiMamba, like RNNs, benefits from its ability to process information recursively over time, updating only a small set of parameters with each iteration, which helps prevent overfitting in scenarios with limited data. Additionally, this framework also avoids the gradient vanishing and explosion issues typically associated with RNNs. Combining these observations with our main results, we can conclude that ConExtBiMamba effectively merges the strengths of MHSA-based models and RNN models.

D. Discussion

As demonstrated in Section V-B, independent Mamba or BiMamba models exhibit low performance in the ASR task, while replacing MHSA with BiMamba layers demonstrates impressive performance and outperforms the vanilla Transformer and Conformer models. Since the latter approach achieves significantly higher ASR performance by additionally employing a feed-forward network (FFN) and a residual connection compared to the independent Mamba and BiMamba models, we then explore the factors contributing to this performance improvement via ablation studies in Table XXI.

TABLE XX: Performance on extremely small dataset AN4 by employing WER (%)

Method/Seed	2048	233	666	1024	3407	Average	Variance
Conformer	4.0	8.2	6.1	4.4	27.4	10.02	77.71
ConExtBiMamba	3.8	3.8	4.8	3.8	6.5	4.54	1.11

TABLE XXI: Ablation Studies on LibriSpeech100 for Transformer and ConExtBiMamba by WER.

Method	dev	test
Transformer	8.0	8.4
Residual	45.7	54.8
- FFN	23.2	25.4
ExtBiMamba	38.5	_{37.7} -
+ Residual	42.1	41.7
+ FFN	34.9	36.1

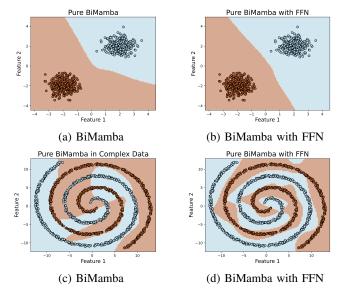


Fig. 3: Decision Boundaries for BiMamba and BiMamba with Feed-forward layer (FFN)

We assume that extracting high-abstraction-level information requires greater nonlinearity than capturing low-abstractionlevel information. Specifically, ASR models transcribe speech signals by understanding the context of acoustic features and aligning speech to tokens, corresponding to low-level sequential and high-level semantic information, respectively. Since a speech enhancement model focuses on low-abstraction-level spectral information, an ASR model may need higher nonlinear ability than a speech enhancement model. As illustrated in Section II, we consider a BiMamba layer as a weakly nonlinear module similar to MHSA [58]. In Figure 3, we use the BiMamba model to find the decision boundary for data with simple and complex distribution, respectively. We observe that BiMamba struggles to find the decision boundary for data of a complex distribution without the aid of an FFN (with ReLU activation similar to that in Transformer), which validates our assumption.

In addition, results in Table XXI indicate the effectiveness of the FFN and residual connection in a Transformer model

for ASR. Similar to independent ExtBiMamba, removing the residual connection and FFN from a Transformer model leads to gradient vanishing and decreases nonlinearity, resulting in significant performance degradation for ASR. This further underpins that using BiMamba layers as a replacement for MHSA is more appropriate for speech tasks which require models to learn high-abstraction-level information than employing it independently.

VI. CONCLUSION

In this paper, we explore the use of Mamba in speech processing, for tasks requiring information from low to high abstraction levels. We first compared two bidirectional designs for Mamba and next employed them independently or as a replacement for MHSA in Transformer and Conformer models. While independent BiMamba models exhibited high performance in the speech enhancement task with the ability to capture lowabstraction-level spectral information, it can not well achieve speech recognition, which requires semantic information within the speech signal. In contrast, using BiMamba as a replacement of MHSA in Conformer (i.e., ConExtBiMamba) matched or exceeded the performance of the SOTA Branchformer across multiple datasets. Ablation studies suggest that using BiMamba to replace MHSA is more appropriate for tasks requiring highabstract-level information due to greater nonlinearity compared to independent BiMamba.

ACKNOWLEDGEMENT

This work was supported by the Australian Research Council Discovery Project DP230101184.

REFERENCES

- A. Vaswani, N. Shazeer, N. Parmar, J. Uszkoreit, L. Jones, A. N. Gomez, Ł. Kaiser, and I. Polosukhin, "Attention is all you need," *Advances in neural information processing systems*, vol. 30, 2017.
- [2] A. Dosovitskiy, L. Beyer, A. Kolesnikov, D. Weissenborn, X. Zhai, T. Unterthiner, M. Dehghani, M. Minderer, G. Heigold, S. Gelly, et al., "An image is worth 16x16 words: Transformers for image recognition at scale," in *International Conference on Learning Representations*, 2020.
- [3] A. Arnab, M. Dehghani, G. Heigold, C. Sun, M. Lučić, and C. Schmid, "Vivit: A video vision transformer," in *Proceedings of the IEEE/CVF international conference on computer vision*, 2021, pp. 6836–6846.
- [4] Z. Liu, Y. Lin, Y. Cao, H. Hu, Y. Wei, Z. Zhang, S. Lin, and B. Guo, "Swin transformer: Hierarchical vision transformer using shifted windows," in *Proceedings of the IEEE/CVF international conference on computer vision*, 2021, pp. 10012–10022.
- [5] J. D. M.-W. C. Kenton and L. K. Toutanova, "Bert: Pre-training of deep bidirectional transformers for language understanding," in *Proceedings* of NAACL-HLT, 2019, pp. 4171–4186.
- [6] X. Liu, Y. Zheng, Z. Du, M. Ding, Y. Qian, Z. Yang, and J. Tang, "Gpt understands, too," AI Open, 2023.
- [7] H. Touvron, L. Martin, K. Stone, P. Albert, A. Almahairi, Y. Babaei, N. Bashlykov, S. Batra, P. Bhargava, S. Bhosale, et al., "Llama 2: Open foundation and fine-tuned chat models," arXiv preprint arXiv:2307.09288, 2023
- [8] L. Dong, S. Xu, and B. Xu, "Speech-transformer: A no-recurrence sequence-to-sequence model for speech recognition," in *Proc. IEEE Int. Conf. Acoust., Speech, Signal Process.*, 2018, pp. 5884–5888.
- [9] A. Gulati, J. Qin, C.-C. Chiu, N. Parmar, Y. Zhang, J. Yu, W. Han, S. Wang, Z. Zhang, Y. Wu, and R. Pang, "Conformer: Convolutionaugmented Transformer for Speech Recognition," in *Proc. Interspeech*, 2020, pp. 5036–5040.
- [10] Y. Peng, S. Dalmia, I. Lane, and S. Watanabe, "Branchformer: Parallel mlp-attention architectures to capture local and global context for speech recognition and understanding," in *International Conference on Machine Learning*. PMLR, 2022, pp. 17627–17643.

- [11] S. Chen, C. Wang, Z. Chen, Y. Wu, S. Liu, Z. Chen, J. Li, N. Kanda, T. Yoshioka, X. Xiao, et al., "Wavlm: Large-scale self-supervised pretraining for full stack speech processing," *IEEE Journal of Selected Topics in Signal Processing*, vol. 16, no. 6, pp. 1505–1518, 2022.
- [12] A. Gu, I. Johnson, K. Goel, K. Saab, T. Dao, A. Rudra, and C. Ré, "Combining recurrent, convolutional, and continuous-time models with linear state space layers," *Advances in neural information processing* systems, vol. 34, pp. 572–585, 2021.
- [13] A. Gu, K. Goel, and C. Re, "Efficiently modeling long sequences with structured state spaces," in *International Conference on Learning Representations*, 2021.
- [14] A. Gupta, A. Gu, and J. Berant, "Diagonal state spaces are as effective as structured state spaces," *Advances in Neural Information Processing* Systems, vol. 35, pp. 22 982–22 994, 2022.
- [15] A. Gu, K. Goel, A. Gupta, and C. Ré, "On the parameterization and initialization of diagonal state space models," *Advances in Neural Information Processing Systems*, vol. 35, pp. 35 971–35 983, 2022.
- [16] A. Gu and T. Dao, "Mamba: Linear-time sequence modeling with selective state spaces," arXiv preprint arXiv:2312.00752, 2023.
- [17] L. Zhu, B. Liao, Q. Zhang, X. Wang, W. Liu, and X. Wang, "Vision mamba: Efficient visual representation learning with bidirectional state space model," arXiv preprint arXiv:2401.09417, 2024.
- [18] Y. Yang, Z. Xing, and L. Zhu, "Vivim: a video vision mamba for medical video object segmentation," arXiv preprint arXiv:2401.14168, 2024.
- [19] O. Lieber, B. Lenz, H. Bata, G. Cohen, J. Osin, I. Dalmedigos, E. Safahi, S. Meirom, Y. Belinkov, S. Shalev-Shwartz, et al., "Jamba: A hybrid transformer-mamba language model," arXiv preprint arXiv:2403.19887, 2024.
- [20] X. Jiang, C. Han, and N. Mesgarani, "Dual-path mamba: Short and long-term bidirectional selective structured state space models for speech separation," arXiv preprint arXiv:2403.18257, 2024.
- [21] K. Li and G. Chen, "Spmamba: State-space model is all you need in speech separation," arXiv preprint arXiv:2404.02063, 2024.
- [22] C. Quan and X. Li, "Multichannel long-term streaming neural speech enhancement for static and moving speakers," arXiv preprint arXiv:2403.07675, 2024.
- [23] H. Li, B. Ma, and K. A. Lee, "Spoken language recognition: from fundamentals to practice," *Proc. IEEE*, vol. 101, no. 5, pp. 1136–1159, 2013.
- [24] A. Gu, T. Dao, S. Ermon, A. Rudra, and C. Ré, "Hippo: Recurrent memory with optimal polynomial projections," *Advances in neural* information processing systems, vol. 33, pp. 1474–1487, 2020.
- [25] D. E. Rumelhart, G. E. Hinton, and R. J. Williams, "Learning internal representations by error propagation, parallel distributed processing, explorations in the microstructure of cognition, ed. de rumelhart and j. mcclelland. vol. 1. 1986," *Biometrika*, vol. 71, pp. 599–607, 1986.
- [26] S. Hochreiter and J. Schmidhuber, "Long short-term memory," *Neural computation*, vol. 9, no. 8, pp. 1735–1780, 1997.
- [27] A. Radford, K. Narasimhan, T. Salimans, I. Sutskever, et al., "Improving language understanding by generative pre-training," 2018.
- [28] Z. Dai, Z. Yang, Y. Yang, J. G. Carbonell, Q. Le, and R. Salakhutdinov, "Transformer-xl: Attentive language models beyond a fixed-length context," in *Proceedings of the 57th Annual Meeting of the Association for Computational Linguistics*, 2019, pp. 2978–2988.
- [29] Q. Zhang, X. Qian, Z. Ni, A. Nicolson, E. Ambikairajah, and H. Li, "A time-frequency attention module for neural speech enhancement," *IEEE/ACM Trans. Audio, speech, Lang. Process.*, vol. 31, pp. 462–475, 2023.
- [30] Q. Zhang, M. Ge, H. Zhu, E. Ambikairajah, Q. Song, Z. Ni, and H. Li, "An empirical study on the impact of positional encoding in transformer-based monaural speech enhancement," in *Proc. IEEE Int. Conf. Acoust.*, Speech, Signal Process., 2024, pp. 1001–1005.
- [31] V. Panayotov, G. Chen, D. Povey, and S. Khudanpur, "Librispeech: an asr corpus based on public domain audio books," in *Proc. IEEE Int.* Conf. Acoust., Speech, Signal Process., 2015, pp. 5206–5210.
- [32] Q. Zhang, X. Qian, Z. Ni, A. Nicolson, E. Ambikairajah, and H. Li, "A time-frequency attention module for neural speech enhancement," *IEEE/ACM Trans. Audio, speech, Lang. Process.*, vol. 31, pp. 462–475, 2023.
- [33] D. Snyder, G. Chen, and D. Povey, "MUSAN: A music, speech, and noise corpus," arXiv preprint arXiv:1510.08484, 2015.
- [34] H. J. Steeneken and F. W. Geurtsen, "Description of the RSG-10 noise database," report IZF, vol. 3, p. 1988, 1988.
- [35] F. Saki and N. Kehtarnavaz, "Automatic switching between noise classification and speech enhancement for hearing aid devices," in in Proc. EMBC, 2016, pp. 736–739.

- [36] F. Saki, A. Sehgal, I. Panahi, and N. Kehtarnavaz, "Smartphone-based real-time classification of noise signals using subband features and random forest classifier," in *Proc. IEEE Int. Conf. Acoust., Speech, Signal Process.*, 2016, pp. 2204–2208.
- [37] Q. Zhang, A. Nicolson, M. Wang, K. K. Paliwal, and C. Wang, "DeepMMSE: A deep learning approach to mmse-based noise power spectral density estimation," *IEEE/ACM Trans. Audio, speech, Lang. Process.*, vol. 28, pp. 1404–1415, 2020.
- [38] J. Salamon, C. Jacoby, and J. P. Bello, "A dataset and taxonomy for urban sound research," in *Proc. ACM-MM*, 2014, pp. 1041–1044.
- [39] D. B. Dean, S. Sridharan, R. J. Vogt, and M. W. Mason, "The QUT-NOISE-TIMIT corpus for the evaluation of voice activity detection algorithms," in *Proc. Interspeech*, 2010.
- [40] G. Hu and D. Wang, "A tandem algorithm for pitch estimation and voiced speech segregation," *IEEE/ACM Trans. Audio, speech, Lang. Process.*, vol. 18, no. 8, pp. 2067–2079, 2010.
- [41] Q. Zhang, H. Zhu, Q. Song, X. Qian, Z. Ni, and H. Li, "Ripple sparse self-attention for monaural speech enhancement," in *Proc. IEEE Int. Conf. Acoust., Speech, Signal Process.*, 2023, pp. 1–5.
- [42] A. Nicolson and K. K. Paliwal, "Masked multi-head self-attention for causal speech enhancement," Speech Com., vol. 125, pp. 80–96, 2020.
- [43] A. Ephrat, I. Mosseri, O. Lang, T. Dekel, K. Wilson, A. Hassidim, W. T. Freeman, and M. Rubinstein, "Looking to listen at the cocktail party: A speaker-independent audio-visual model for speech separation," arXiv preprint arXiv:1804.03619, 2018.
- [44] D. P. Kingma and J. Ba, "Adam: A method for stochastic optimization," arXiv preprint arXiv:1412.6980, 2014.
- [45] R. I.-T. P. ITU, "862.2: Wideband extension to recommendation P. 862 for the assessment of wideband telephone networks and speech codecs. ITU-Telecommunication standardization sector, 2007."
- [46] J. Jensen and C. H. Taal, "An algorithm for predicting the intelligibility of speech masked by modulated noise maskers," *IEEE/ACM Trans. Audio,* speech, Lang. Process., vol. 24, no. 11, pp. 2009–2022, 2016.
- [47] Y. Hu and P. C. Loizou, "Evaluation of objective quality measures for speech enhancement," *IEEE Trans. Audio, Speech, Lang. process.*, vol. 16, no. 1, pp. 229–238, 2007.
- [48] A. Acero and R. M. Stern, "Environmental robustness in automatic speech recognition," in *Proc. IEEE Int. Conf. Acoust., Speech, Signal Process.* IEEE, 1990, pp. 849–852.
- [49] D.-C. Lyu, T.-P. Tan, E. S. Chng, and H. Li, "Seame: a mandarin-english code-switching speech corpus in south-east asia," in *Eleventh Annual Conference of the International Speech Communication Association*, 2010
- [50] X. Shi, Q. Feng, and L. Xie, "The asru 2019 mandarin-english codeswitching speech recognition challenge: Open datasets, tracks, methods and results," arXiv preprint arXiv:2007.05916, 2020.
- [51] Z. Zeng, Y. Khassanov, V. T. Pham, H. Xu, E. S. Chng, and H. Li, "On the end-to-end solution to mandarin-english code-switching speech recognition," in *Proc. Interspeech*, 2019, pp. 2165–2169.
- [52] H. Liu, X. Zhang, L. P. Garcia, A. W. Khong, E. S. Chng, and S. Watanabe, "Aligning speech to languages to enhance code-switching speech recognition," arXiv preprint arXiv:2403.05887, 2024.
- [53] S. Watanabe, T. Hori, S. Karita, T. Hayashi, J. Nishitoba, Y. Unno, N. Enrique Yalta Soplin, J. Heymann, M. Wiesner, N. Chen, A. Renduchintala, and T. Ochiai, "ESPnet: End-to-end speech processing toolkit," in *Proc. Interspeech*, 2018, pp. 2207–2211.
- [54] Z. Kong, W. Ping, A. Dantrey, and B. Catanzaro, "Speech denoising in the waveform domain with self-attention," in *Proc. IEEE Int. Conf. Acoust., Speech, Signal Process.*, 2022, pp. 7867–7871.
- [55] H. Liu, H. Xu, L. P. Garcia, A. W. H. Khong, Y. He, and S. Khudanpur, "Reducing language confusion for code-switching speech recognition with token-level language diarization," in *Proc. IEEE Int. Conf. Acoust.*, *Speech, Signal Process.*, 2023, pp. 1–5.
- [56] H. Liu, L. P. Garcia, X. Zhang, A. W. Khong, and S. Khudanpur, "Enhancing code-switching speech recognition with interactive language biases," in *Proc. IEEE Int. Conf. Acoust., Speech, Signal Process.* IEEE, 2024, pp. 10886–10890.
- [57] P. Koehn, Neural machine translation. Cambridge University Press, 2020.
- [58] C. Manning, "Lecture 8: Transformers," CS224N: Natural Language Processing with Deep Learning, Stanford University, 2024, accessed: 2024-05-14, Slide 32. [Online]. Available: https://web.stanford.edu/class/ cs224n/slides/cs224n-spr2024-lecture08-transformers.pdf